# Dinuclear Gold Complexes Supported by Wide Bite Angle Diphosphines for Preorganization-Induced Selective Dual-Gold Catalysis

Lankelma, M.; Vreeken, V.; Siegler, M.A.; van der Vlugt, J.I.

**DOI**
10.3390/inorganics7030028

**Publication date**
2019

**Document Version**
Final published version

**Published in**
Inorganics

*inorganics*

MDPI

*Article*

# Dinuclear Gold Complexes Supported by Wide Bite Angle Diphosphines for Preorganization-Induced Selective Dual-Gold Catalysis

**Marianne Lankelma [1], Vincent Vreeken [1], Maxime A. Siegler [2] and Jarl Ivar van der Vlugt [1,*]**

[1] Homogeneous, Supramolecular, and Bio-inspired Catalysis, van 't Hoff Institute for Molecular Sciences, University of Amsterdam, Science Park 904, 1098 XH Amsterdam, The Netherlands; m.i.lankelma@uva.nl (M.L.); vincent.vreeken@gmail.com (V.V.)

[2] Small Molecule X-ray Laboratory, Department of Chemistry, Johns Hopkins University, Baltimore, MD 21218, USA; xray@jhu.edu

* Correspondence: j.i.vandervlugt@uva.nl; Tel.: +31-20-5256459

Received: 29 January 2019; Accepted: 20 February 2019; Published: 26 February 2019


**Abstract:** The synthesis, reactivity, and potential of well-defined dinuclear gold complexes as precursors for dual-gold catalysis is explored. Using the preorganizing abilities of well-known wide bite angle diphosphine ligands, DBFPhos and DPEPhos, dinuclear Au(I)–Au(I) complexes **1** and **2** are used as precursors to form well-defined monocationic species with either a chlorido- or acetylido-ligand bridging the two gold centers. These compounds are active catalysts for the dual-gold heterocycloaddition of a urea-functionalized alkyne, and the preorganization of both Au-centers affords efficient σ,π-activation of the substrate, even at high dilution, significantly outperforming benchmark mononuclear catalysts.

**Keywords:** dinuclear gold complex; wide bite-angle diphosphine ligand; dual-gold catalysis; bridging acetylide; σ,π-activation

## 1. Introduction

Recently, the catalytic activation of substrates using two gold centers has proven to be a valuable strategy for a wide range of transformations in the broader context of gold-mediated catalysis [1–14]. Commonly, mono-gold catalysis relies on π-activation of a substrate (e.g., an alkene) by a cationic Au(I) center. Dual-gold catalysis, on the other hand, can lead to both σ- and π-activation (either of the same functional group within a substrate or of two separate functional groups) by two Au centers. The proximity of both Au-centers has occasionally been credited to enhance reactivity [15–17]. The prevailing strategy utilizes mononuclear Au(I) complexes to induce this mode of activation (Scheme 1) [18]. However, this approach offers no handles to induce preorganization of both Au-centers to specifically target well-defined σ,π-activation of, for example, C–C multiple bonds whilst avoiding π- or simultaneous σ- and π-coordination (one mode per Au-center), nor does it provide any control over the selective binding of bifunctional substrates (e.g., for heterocyclizations). We have recently reported the catalytic competence of well-defined dinuclear σ,π-alkynide complexes in dual-gold catalysis, highlighting the importance of two preorganized Au centers with respect to regioselectivity and activity for intramolecular hydroamination [19,20]. This was achieved using the ditopic tridentate ligand $\mathbf{PN^HP^{iPr}}$ (2,2′-bis(diisopropylphosphino)-4,4′-ditolylamine) (Figure 1). However, under certain (catalytically relevant) conditions, the redox-active nature of this scaffold induced significant structural rearrangement of the ligand backbone, giving rise to a carbazolyl-based derivative. In order to eliminate such ligand-centered chemistry leading to structural reorganization, and to exploit more readily available diphosphine ligands, we investigated wide bite angle diphosphine ligands with

ether backbones [21–29]. Basic coordination chemistry of these potentially dinucleating ligands toward gold has already been established by several groups [30–32]. Furthermore, Koshevoy et al. investigated the formation and photochemical properties of bis-gold complexes with the related ligand Xantphos [33–38].

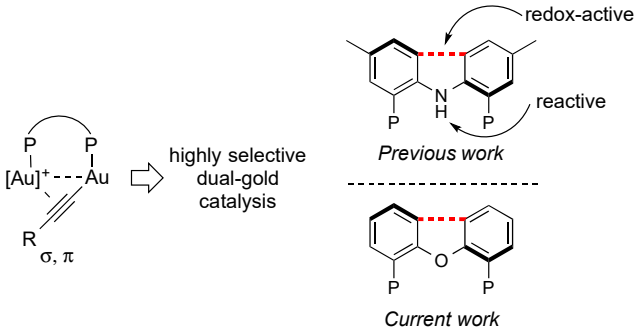


**Figure 1.** Left: Strategy for the preorganization of two gold-centers for σ–π-coordination of hydrocarbon π-systems using a diphosphine platform. Right: previous and current work on bis-gold chemistry with specific diphosphine ligands.

We herein report on the formation of μ-chlorido and σ,π-alkynide derivatives of $Au_2Cl_2(\kappa^2$-*P*;*P*-DBFPhos) and $Au_2Cl_2(\kappa^2$-*P*;*P*-DPEPhos) and catalytic activity of these well-defined dinuclear species vs. mononuclear benchmarks in the intramolecular hydroamidation of functionalized amido-alkenes. This study emphasizes the positive effect of preorganization of two gold centers for reactions that proceed via simultaneous σ- and π-activation of a carbon-based π-system in a substrate. This effect is illustrated via a dilution study with mono- and di-nuclear catalysts.

## 2. Results and Discussion

The straightforward reaction of **L1** (DBFPhos) and **L2** (DPEPhos) with $AuCl(SMe_2)$ in a 1:2 ratio provided white solids **1** ($^{31}$P NMR: δ 23.3) and **2** ($^{31}$P NMR: δ 21.6). The respective $^1$H NMR spectra were suggestive of $C_2$ symmetric species (Scheme 1). Single crystals suitable for X-ray structure determination of **2** were obtained by slow vapor diffusion of acetone into a solution of **2** in $CHCl_3$ (Figure 2), while for **1** only a connectivity plot could be reliably obtained (from single crystals grown from $CH_2Cl_2$–pentane; see Section 3, materials and methods). Complex **2** displays an aurophilic $d^{10}$–$d^{10}$ interaction [39–41] with an intramolecular Au1···Au2 distance of 3.0116(4) Å, while in **1** this Au···Au distance was approximately 7.57 Å. It should be noted that these structures complement known ones for both compounds, with different (amounts and/or combinations of) lattice solvents present [30,31].

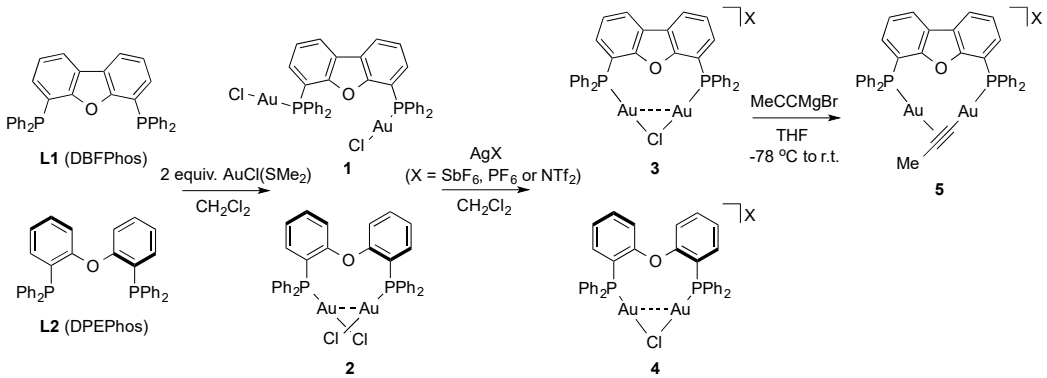


**Scheme 1.** Synthesis of well-defined $Au_2$-complexes **3**–**5** from Au(I)–Au(I) precursors **1** and **2**, generated by reaction of ligands **L1** and **L2** with 2 equivalent of $AuCl(SMe_2)$.

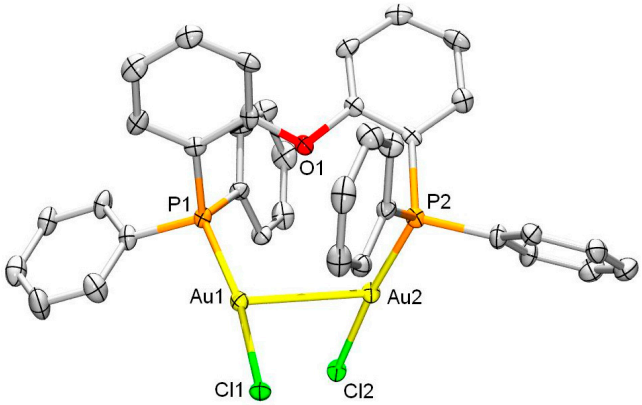


**Figure 2.** Displacement ellipsoid plots (50% probability level) of **2**. The disordered mixture of lattice $CHCl_3$ and acetone molecules in the asymmetric unit, as well as the hydrogen atoms, have been omitted for clarity. Selected bond lengths (Å) and angles (°): Au1–P1 2.2393(17); Au2–P2 2.2441(18); Au1–Cl11 2.3122(15); Au2–Cl2 2.3419(15); Au1···Au2 3.0116(4); P1–Au1–Cl1 168.48(6); P2–Au2–Cl2 173.97(7).

When exploiting a gold-halide precursor for gold-mediated catalysis, a prerequisite is the generation of a vacant coordination site via halide abstraction. Addition of one equivalent of $AgNTf_2$ or related silver salts such as $AgSbF_6$ or $AgPF_6$ to **1** or **2** led to new species **3** and **4**, respectively, according to $^{31}P$ NMR spectroscopy, with signals at δ 15.6 and 20.1 ppm, respectively. The relatively large difference in the $^{31}P$ chemical shifts observed for **1** and **3** may be related to significant reorientation of the phosphorus atoms upon formation of the single halide bridgehead. Single crystals suitable for X-ray structure determination were obtained by layer-diffusion of pentane into a $CH_2Cl_2$ solution of complex **3**. The resulting molecular structure (Figure 3) shows that both gold centers were bridged by a single chlorido ligand, leading to an acute ∠Au1–Cl1–Au2 of 78.79(7)°. Relative to "open" complex **1**, the intramolecular Au···Au distance in **3** was significantly decreased (Δd ± 4.58 Å) due to increased directional positioning of the phosphorus lone pairs, despite the large natural bite angle. To the best of our knowledge, the existence of a single chlorido bridgehead between two $Au^I$ centers is relatively rare [42–48]. Notably, this is only the second example of an intramolecular Au–Cl–Au bridge stabilized by a single dinucleating ligand, the first being our work with the ligand $\mathbf{PN^HP^{iPr}}$. Attempts to characterize complex **4** via X-ray crystallography unfortunately failed, but spectroscopic data support formulation of this species as $[Au_2(\mu\text{-Cl})(\kappa^2\text{-}P,P\text{-DPEPhos})]^+$.

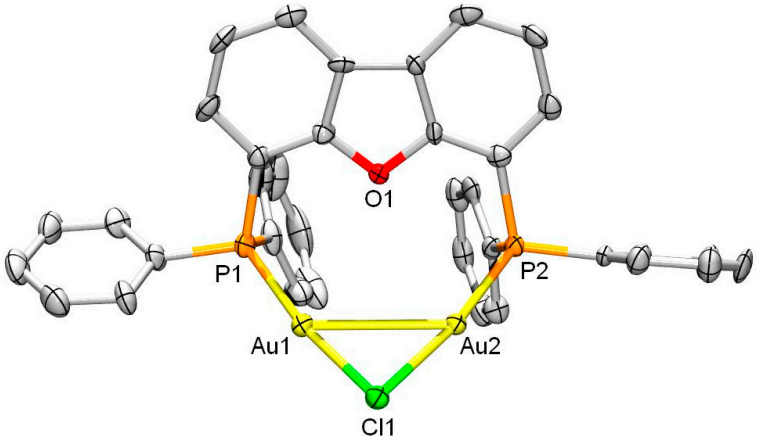


**Figure 3.** Displacement ellipsoid plot (50% probability level) of one of the two crystallographically independent cationic parts of **3**. The $SbF_6$ counterion and hydrogen atoms have been omitted for clarity. Selected bond lengths (Å) and angles (°) (only given for the Au1–Au2 cationic part): Au1–P1A 2.236(2); Au1–Cl1A 2.353(2); Au1···Au2 2.9871(5); P1A–Au1–Cl1A 172.20(8); P2A–Au2–Cl1A 174.13(9); Au1–Cl1A–Au2 78.79(7).

Complex **3** was amenable to reaction with 1-propynylmagnesium bromide, forming σ,π-coordinated alkynide-bridging complex **5**, akin to our previous report using the $\mathbf{PN^HP^{iPr}}$ scaffold. The $^{31}$P NMR spectrum of **5** displayed a singlet at 23.8 ppm and the elemental composition as $[Au_2(\mu\text{-CCMe})(\kappa^2\text{-}P,P\text{-DBFPhos})]^+$ was corroborated by high-resolution electron spray ionization mass spectrometry (ESI-MS). X-ray structure determination of a minute amount of adventitious crystalline material obtained from cyclopentane-$CHCl_3$ showed direct evidence of the dual interaction of the –C≡CMe ligand with both gold centers (i.e., σ-coordination of the terminal C37 carbon to Au2 and π-coordination of the triple bond to Au1; Figure 4). To the best of our knowledge, this is only the second crystallographically-characterized intramolecular $Au_2$(σ,π-acetylide) complex supported by a diphosphine ligand, and an illustration that preorganization of two gold centers may lead to selective σ,π-coordination of the alkyne moiety. Complex **4** is envisioned to initially react with 1-propynylmagnesium bromide in a similar fashion to provide putative complex **6**, postulated as $[Au_2(\mu\text{-CCMe})(\kappa^2\text{-}P,P\text{-DPEPhos})]^+$. However, this species and analogues generated by using 4-ethynyl-α,α,α-trifluorotoluene proved to be highly sensitive to water, precluding its spectral characterization.

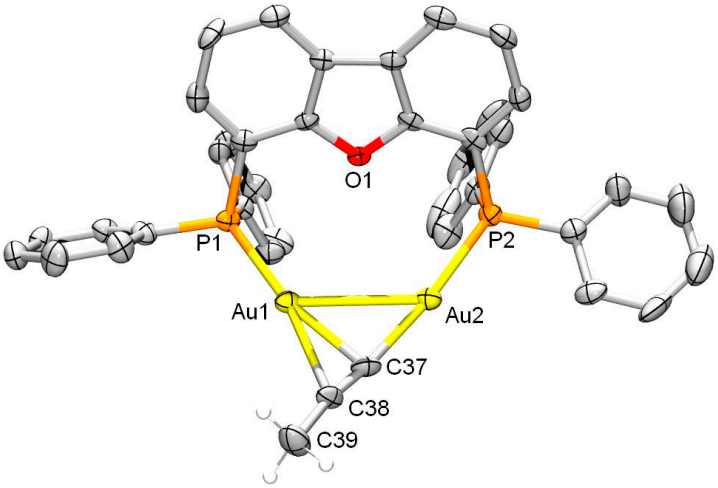


**Figure 4.** Displacement ellipsoid plot (50% probability level) for **5**, $[Au_2(\mu\text{-CCMe})(\kappa^2\text{-}P,P\text{-DBFPhos})]^+$. Two lattice cyclopentane solvent molecules, the $SbF_6$ counterion and hydrogen atoms, except for those on C39, have been omitted for clarity. Selected bond lengths (Å) and angles (°): P1–Au 2.243(2); P2–Au2 2.267(2); Au1–Ct(C37–C38) 2.236; Au2–C37 2.055(9); C37–C38 1.18(1); C38–C39 1.45(1); Au1···Au2 2.9951(8); P1–Au1–Ct(C37–C38) 175.09; P2–Au2–C37 170.4(2); C37–C38–C39 169.3(10).

Having established that ligands **L1** and **L2** can facilitate pre-activation of C≡C bonds in a σ,π-fashion, we wondered about their activity in the heterocyclization (intramolecular hydroamination) of urea-functionalized alkyne **A**. Previously, Paradies and co-workers compared AuCl(Xantphos), $Au_2Cl_2$(Xantphos), and $AuCl(PPh_3)$ for the intermolecular hydroamidation of cyclohexene (and analogs thereof) and toluene sulfonamide in the presence of stoichiometric amounts of silver salts as halide abstracting agents [17]. This study concluded that $[Au_2(Xantphos)]^{2+}$ and the corresponding species $[Au_2(Xantphos)_2]^{2+}$, which forms from the former, were both catalytically inactive.

We were curious whether dinuclear σ,π-activation could result in anti-Markovnikov hydroamidation of substrate **A** (Scheme 2). This reaction was previously reported by Medio-Simón and co-workers to form five-membered indole **B** via σ,π-activation, using two equivalents of the mononuclear gold complex $AuCl(P^tBu_3)$ as the best catalyst [49]. Using 2.5 mol % of either dihalide precursors **1** or **2** with two equiv. of $AgSbF_6$, or species **3** or **4** with one equiv. of $AgSbF_6$, in *N*,*N*′-DMF at 60 °C for 5 h led to full conversion and high regioselectivity to **B** (95–100%), as determined by $^1$H NMR spectroscopy, in accordance with a selective σ,π-acetylide mechanism. All four $Au_2$

systems outperformed the mononuclear benchmark AuCl($P^tBu_3$) in the presence of one equiv. of $AgSbF_6$ (80% **B**). When no $AgSbF_6$ was added, significantly lower regioselectivity and conversion was observed for each system, presumably due to slower generation of the σ,π-acetylide species. The high regioselectivity achieved with these dinuclear catalysts is attributed to the ligand-enforced proximity of the two Au(I) centers. High resolution mass spectra of 1:1 mixtures of **3** or **4** (with or without additional $AgSbF_6$) and substrate **A**, measured ten minutes after dissolution of the two solids in DMF, suggested formation of σ,π-complexes with formal loss of HCl.

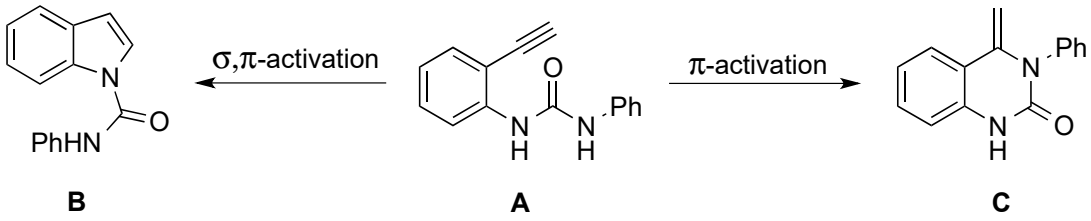


**Scheme 2.** Heterocyclization of 1-(ethynylphenyl)urea (**A**) to either anti-Markovnikov product (**B**) or Markovnikov addition product (**C**).

We hypothesized that the high local concentration of gold(I) centers provided by these dinuclear gold complexes should render the regioselectivity of the complexes independent of the catalyst loading [50,51]. Dilution studies to investigate the effect of decreased catalyst loadings on the level of regiocontrol for the conversion of **A** to **B** and **C** clearly validated this hypothesis, as the consistently high regioselectivity to **B** with catalyst **4** in the presence of one equivalent of $AgSbF_6$ was not dependent on the concentration of gold centers (ranging from 5 to 0.5 mol %) (Figure 5). In contrast, dilution experiments with mononuclear AuCl($P^tBu_3$) in the presence of an equimolar amount of $AgSbF_6$ resulted in a sharp drop in selectivity, particularly below 1 mol % of catalyst loading, to around 40% yield of **B** [52]. These results demonstrate the benefits of well-defined pre-organization of two gold centers to enforce selective σ,π-activation and to mediate regioselective dual-gold catalysis with functionalized alkynes, even at low catalyst loadings.

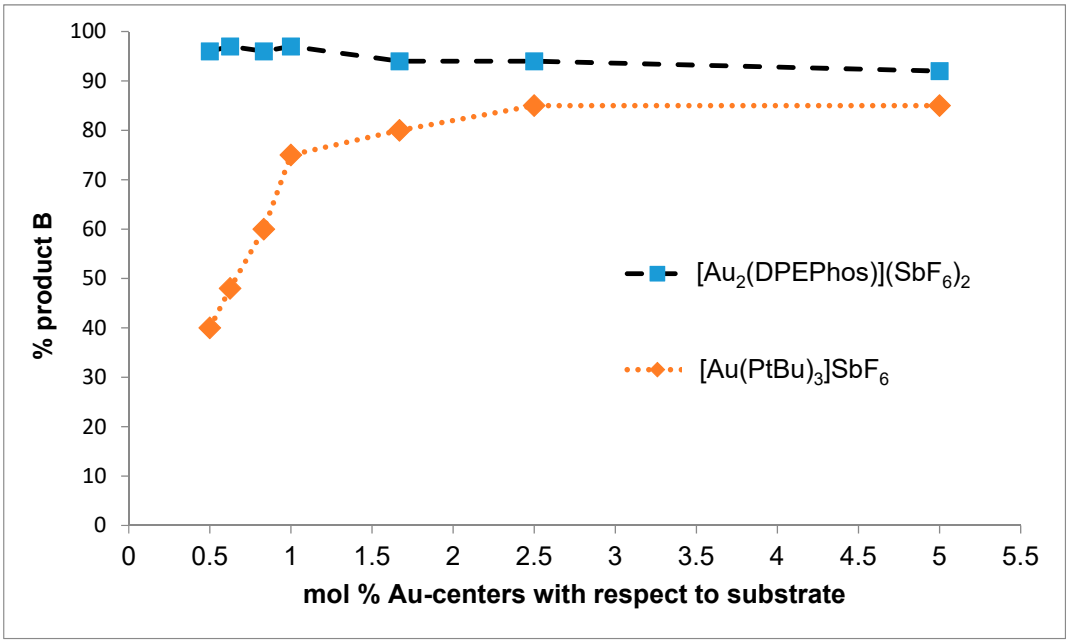


**Figure 5.** Comparison of regioselectivity to indole **B** under various dilution conditions, obtained with dinuclear catalyst **4** in the presence of one equiv. of $AgSbF_6$ vs. mononuclear benchmark AuCl($P^tBu_3$) with one equiv. $AgSbF_6$.

Encouraged by this proof-of-concept demonstration of ligand-induced preorganization of two gold centers for dual-gold catalysis, we explored the structurally related substrate **D** featuring an additional methylene unit between the phenyl ring and the urea fragment (Scheme 3, reaction I). This substrate was quantitatively converted via selective 6–*endo*-dig cyclization to yield product **E** when using pre-activated dinuclear catalyst **3** or **4** in the presence of $AgSbF_6$. Substrate **F**, the thiourea-derivative of substrate **A**, did not provide the corresponding *N*-phenyl-1*H*-indole-1-carbothioamide. Instead, product **G** was selectively obtained via 6-*exo*-dig cyclization (Scheme 3, reaction II), which is in line with observations by Shi et al., who speculated on σ,π-activation of a propargylic thiourea and subsequent *N*-attack to obtain the same type of cyclic 6-membered compound [53]. Finally, unlike the complex $[Au_2(BIPHEP)](NTf_2)_2$ [54], which despite its dinuclear nature cannot accommodate σ,π-coordination because of steric constraints, digold complexes **3** and **4** do not dimerize 2-ethynylaniline but rather induced selective cyclization to form indole **H** (Scheme 3, reaction III), suggesting that σ,π-coordination of one molecule of 2-ethynylaniline was energetically more favorable than σ-coordination of two molecules of 2-ethynylaniline with wide bite angle diphosphine frameworks that do allow bridging ligation of acetylenic substrates.

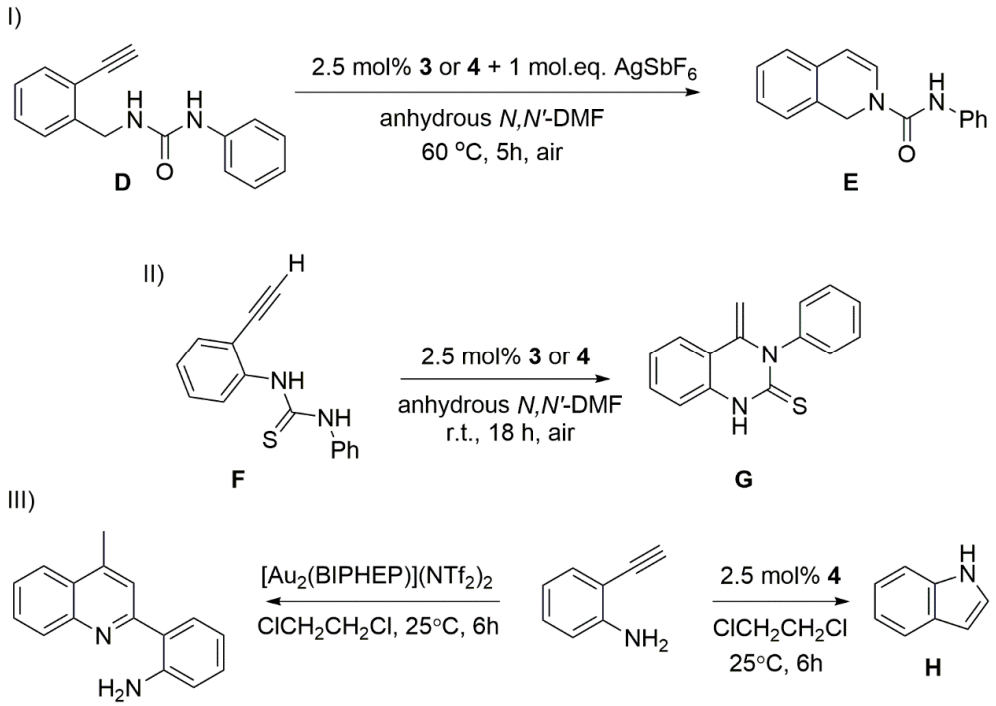


**Scheme 3.** Other catalytic reactions with complexes **3** and **4** with (thio)urea-containing phenylacetylenic substrates **D**, **F,** and 2-ethynylaniline to support the σ,π-activation of acetylenic substrates.

## 3. Materials and Methods

### *3.1. General Comments*

$P(^tBu)_3AuCl$, $AgSbF_6$, $AgNTf_2$, and 1-propynylmagnesium bromide (0.5 M in THF) were purchased from commercial suppliers and used without further purification. Compound **A** was prepared according to a literature procedure [49]. $AuCl(SMe_2)$ was either purchased from Sigma Aldrich (St. Louis, MO, USA) or synthesized by reacting $HAuCl_4.3H_2O$ with an excess of dimethylsulfide in ethanol at room temperature for ten minutes. 1-Propynylmagnesium bromide was titrated in triplo with $I_2$/LiCl in THF. Tetrahydrofuran and pentane were distilled from sodium benzophenone ketyl. Dichloromethane was distilled from $CaH_2$. All reactions were carried out in flame-dried or oven-dried glassware under a nitrogen atmosphere, unless otherwise stated. Flash column chromatography was performed with silica gel (Screening Devices, 60Å, particle size

0.040–0.063 μm). Eluent mixtures are reported as *v/v* %. Products were visualized by UV light. NMR spectra ($^{1}$H, $^{31}$P{$^{1}$H}, $^{13}$C{$^{1}$H}) were measured at room temperature on Bruker DRX 500, AV 400, DRX 300 and AV 300 instruments (Bruker, Billerica, MA, USA) and referenced against $SiMe_4$, external $H_3PO_4$ or solvent. NMR chemical shifts are reported in ppm, coupling constants (J) are reported in Hertz. High resolution mass spectra were recorded on a JEOL AccuTOF LC JMS-T100LP mass spectrometer (JEOL, Tokyo, Japan) using electron spray ionization (ESI) or field desorption (FD). GC-MS spectra were recorded on an Agilent 5973 Network Mass Selective Detector (Agilent, Santa Clara, CA, USA) equipped with a 6890N Network GC System.

### *3.2. Syntheses of New Complexes*

**Complex 1, $Au_2Cl_2$(DBFPhos).** DBFPhos (1 equiv.) and AuCl($SMe_2$) (2 equiv.) were dissolved in $CH_2Cl_2$ and stirred at room temperature for a couple of hours, depending on the scale. The resultant white suspension was concentrated to ca. 0.5 mL. Pentane (20 mL) was added, leading to formation of a white precipitate. The suspension was stirred vigorously for 5 min, after which the precipitate was allowed to settle. The colorless supernatant was removed and the residue was dried under vacuum, yielding **1** as a white solid in quantitative yield. Single crystals suitable for X-ray diffraction were obtained by layering ca. 1.5 mL of pentane on top of a solution of ca. 4 mg of complex **1** in ca. 0.3 mL of $CH_2Cl_2$ in a 2 mL vial. $^{31}$P{$^{1}$H} NMR (202 MHz, $CD_2Cl_2$, ppm): δ 23.3 (s). $^{1}$H NMR (500 MHz, $CD_2Cl_2$, ppm): δ 8.23 (d, *J* = 7.7 Hz, 2H), 7.56–7.51 (m, 12H), 7.48–7.42 (m, 10H), 7.15 (dd, *J* = 13.4, 7.6 Hz, 2H). $^{13}$C{$^{1}$H} NMR (126 MHz, $CD_2Cl_2$, ppm): δ 156.5 (d, *J* = 4.2 Hz), 134.3 (d, *J* = 14.6 Hz), 133.1 (d, *J* = 7.4 Hz), 132.5 (s), 129.4 (d, *J* = 12.3 Hz), 127.8 (s), 127.3 (s), 124.8 (br. s), 124.4 (d, *J* = 5.5 Hz), 124.2 (d, *J* = 9.5 Hz). HR-MS (ESI) calcd. for $[M - Cl]^+$ $C_{36}H_{26}Au_2ClOP_2$ *m/z*: 965.0478, found 965.0463.

**Complex 2, $Au_2Cl_2$(DPEPhos).** DPEPhos (1 equiv.) and AuCl($SMe_2$) (2 equiv.) were dissolved in $CH_2Cl_2$ and stirred at room temperature for several hours. The resultant white suspension was concentrated to ca. 0.5 mL. Pentane (20 mL) was added, leading to formation of a white precipitate. The resultant suspension was stirred vigorously for 5 min, after which the precipitate was allowed to settle. The colorless supernatant was removed and the white residue was dried under vacuum, yielding **2** as a white solid in yields around 75%. Single crystals suitable for X-ray diffraction (transparent needles) were obtained by slow vapor diffusion of acetone into a solution of complex **2** in $CHCl_3$. $^{31}$P{$^{1}$H} NMR (162 MHz, $CD_2Cl_2$, ppm): δ 21.6 (s). $^{1}$H NMR (400 MHz, $CD_2Cl_2$, ppm): δ 7.61–7.27 (m, 18H), 7.24–7.12 (m, 6H), 7.05 (dd, *J* = 8.3, 5.3 Hz, 2H), 6.83-6.69 (m, 2H). $^{13}$C{$^{1}$H} NMR (101 MHz, $CD_2Cl_2$, ppm): δ 134.9 (d, *J* = 14.4 Hz), 134.1 (d, *J* = 5.3 Hz), 138.9, 133.4 (d, *J* = 14.0 Hz), 132.0 (d, *J* = 2.3 Hz), 131.2 (d, *J* = 2.7 Hz), 129.6 (d, *J* = 12.3 Hz), 129.2 (d, *J* = 12.1 Hz), 124.8 (d, *J* = 9.1 Hz), 120.0 (d, *J* = 4.9 Hz). HR-MS (ESI) calcd. for $[M - Cl]^+$ $C_{36}H_{28}Au_2ClOP_2$ *m/z*: 967.0635, found 967.0604.

**Complex 3, [$Au_2$(μ-Cl)(DBFPhos)](X).** Inside a nitrogen-filled glovebox, $AgSbF_6$ or $AgNTf_2$ (1 equiv.) was added to complex **1** (1 mol. equiv.) and the reaction vessel was covered in aluminum foil. In air, the mixture was suspended in $CH_2Cl_2$ or THF and the suspension was stirred for several hours. The reaction mixture was filtered over 2–3 cm of Celite on top of a frit filter, and the filtrate was evaporated until dry to yield complex **3** as a white solid. Colorless single crystals suitable for X-ray diffraction of the triflimide derivative were obtained by layering ca. 1.5 mL of pentane on top of a solution of ca. 4 mg of complex **3** in ca. 0.5 mL of $CH_2Cl_2$ in an NMR-tube. $^{31}$P{$^{1}$H} NMR (121 MHz, $CD_2Cl_2$, ppm): δ 15.6 (s). $^{1}$H NMR (300 MHz, $CD_2Cl_2$, ppm): δ 8.36 (d, *J* = 7.8 Hz, 2H), 7.65–7.30 (m, 22H), 7.02 (dd, *J* = 12.5, 7.6 Hz, 2H). $^{13}$C{$^{1}$H} NMR (75 MHz, $CD_2Cl_2$, ppm): δ 157.1 (d, *J* = 5.8 Hz), 134.2 (d, *J* = 14.3 Hz), 133.6 (d, *J* = 2.5 Hz), 131.9 (s), 130.1 (d, *J* = 12.8 Hz), 126.3 (s), 125.2 (d, *J* = 8.7 Hz), 124.7 (d, *J* = 5.4 Hz), 124.3 (s), 122.4 (s), 118.1 (s), 113.9 (s), 112.3 (s), 111.5 (s). HR-MS (ESI) calcd. for $[M]^+$ $C_{36}H_{26}Au_2ClOP_2$ *m/z*: 965.0478, found 965.0497.

**Complex 4 [$Au_2$(μ-Cl)(DPEPhos)]($SbF_6$).** Inside a glovebox, $AgSbF_6$ (or a related Ag-salt; 1 mol. equiv.) was added to complex **2** and the reaction vessel was covered in aluminum foil. In air, the mixture was suspended in $CH_2Cl_2$ or THF and the suspension was stirred for a couple of hours.

The reaction mixture was filtered over ca. 1 cm of Celite on top of a frit filter and the filtrate was evaporated until dry to yield complex **4** as a white solid (average yield 81%). All attempts to grow single crystals of complex **4** failed. $^{31}P\{^{1}H\}$ NMR (121 MHz, $CD_2Cl_2$, ppm): δ 20.1 (s). $^{1}H$ NMR (300 MHz, $CD_2Cl_2$, ppm): δ 7.66–7.35 (m, 24H), 7.13 (t, *J* = 7.6 Hz, 2H), 6.83 (ddd, *J* = 12.7, 7.8, 1.4 Hz, 2H). $^{13}C\{^{1}H\}$ NMR (75 MHz, $CD_2Cl_2$, ppm): δ 160.1 (d, *J* = 1.5 Hz), 152.2 (d, *J* = 6.9 Hz), 136.9, 136.3 (d, *J* = 2.2 Hz), 136.0, 134.4, 133.0, 132.0 (d, *J* = 2.8 Hz), 131.5 (d, *J* = 9.3 Hz), 129.6, 128.8 (d, *J* = 11.7 Hz), 128.1, 121.2 (d, *J* = 2.5 Hz), 120.9 (d, *J* = 3.8 Hz). HR-MS (ESI) calcd. for $[M]^+$ $C_{36}H_{28}Au_2ClOP_2$ *m/z*: 967.0635, found 967.0664.

**Complex 5, [$Au_2$(μ-propynyl)(DBFPhos)]($SbF_6$).** Complex **3SbF$_6$** was dissolved in THF and the Schlenk was covered in aluminum foil. At −78 °C, a 0.5 M solution of 1-propynylmagnesium bromide in THF (1 equiv.) was added and the resultant orange solution was stirred for ca. 15 min at −78 °C followed by 5 h at room temperature. The reaction mixture was quenched with a saturated aqueous solution of $NaHCO_3$ and the product was extracted three times into $CH_2Cl_2$. The aqueous layer was extracted two times with $CH_2Cl_2$. The combined organic layers were dried over $MgSO_4$ and the solvent was removed under reduced pressure. Sonication with toluene was then performed for 30 min, followed by filtration over paper, and concentration of the filtrate afforded **5** as a white solid. Single crystals (tiny transparent needles) suitable for X-ray diffraction were obtained by layering ca. 1.5 mL of cyclopentane on top of a solution of ca. 4 mg of complex **5** (in its orange form) in ca. 0.3 mL of $CHCl_3$ in a 2 mL vial. $^{31}P\{^{1}H\}$ NMR (162 MHz, $CD_2Cl_2$, ppm): δ 23.8 (s). HR-MS (ESI) calcd. for $[M]^+$ $C_{39}H_{29}Au_2OP_2$ *m/z*: 969.1025, found 969.1513 for the crude solid.

### *3.3. General Information on Catalytic Studies*

**Synthesis of Substrate D.** A solution of (2-ethynylphenyl)methanamine, prepared following a literature procedure [55], (0.84 g, 6.40 mmol) in $CH_2Cl_2$ (16 mL) was added to phenyl isocyanate (695 μL, 6.40 mmol). The resultant red suspension was "stirred" for ca. 1.5 h (formation of a solid soon impeded stirring) before being added to a second batch of phenyl isocyanate (695 μL, 6.40 mmol) and stirred for ca. 16 h. The resultant brown suspension was concentrated, impregnated on silica, and purified by column chromatography (ca. 30 cm of silica gel, Ø NS 29/32, hexane/ethyl acetate 3:1) to yield **D** as a beige solid (0.92 g, 57% yield). $^{1}H$ NMR (300 MHz, acetone-$d_6$, ppm): δ 8.11 (br s, 1H), 7.54–7.08 (m, 8H), 6.91 (t, *J* = 7.0 Hz, 1H), 6.25 (br s, 1H), 4.58 (d, *J* = 5.9 Hz, 2H), 3.94 (s, 1H). HR-MS (ESI) calcd. for [M + H]+ $[C_{16}H_{14}N_2O + H]+$ *m/z*: 251.1184, found 251.1199.

**Synthesis of Substrate F.** To $CH_2Cl_2$ (2 mL) was added 2-ethynylaniline (142 μL, 1.25 mmol) and phenyl isothiocyanate (150 μL, 1.25 mmol). The mixture was stirred for 30 min at room temperature and then heated to reflux for 4 h. The solution was allowed to cool down to room temperature and all volatiles were removed, yielding a light orange solid that was dried under vacuum. The crude product was impregnated on silica and purified by column chromatography (ca. 28 cm of silica gel, Ø NS 29/32, hexane/ethyl acetate 3:1, Rf 0.38) to yield substrate F (202 mg, 64%). $^{1}H$ NMR (300 MHz, $CDCl_3$, ppm): δ 8.55 (d, *J* = 8.3 Hz, 1H), 8.30 (br s, 1H), 7.91 (br s, 1H), 7.57–7.35 (m, 7H), 7.12 (t, *J* = 7.2 Hz, 1H), 3.09 (s, 1H). HR-MS (FD) calcd. for [M]+ $C_{15}H_{12}N_2S$ *m/z*: 252.0721, found 252.0718.

**General Procedure for Catalytic Studies with Substrates A, D and F.** An oven-dried 4 mL vial was charged with the substrate (50 μmol) and a digold complex (2.5 mol %; 1.25 μmol). The solids were dissolved in anhydrous *N,N′*-DMF (0.5 mL) and stirred in air at 60 °C for 5 h. If $AgSbF_6$ was added, this was done either by addition of the dry solid inside a nitrogen-filled glovebox or by addition of a stock solution of $AgSbF_6$ in *N,N′*-DMF. The reaction mixture was transferred to a round-bottom flask with $CH_2Cl_2$ or $CHCl_3$ and all solvent was evaporated under reduced pressure. NMR spectra were recorded in $CDCl_3$ or acetone-$d_6$.

**General Procedure for Dilution Studies.** The general procedure for catalysis was applied in seven experiments, each comprising a different catalyst loading. For the dilution studies on

$[Au_2(DPEPhos)](SbF_6)_2$, **4** and $AgSbF_6$ were each added in 2.5 mol %, 1.25 mol %, 0.835 mol %, 0.5 mol %, 0.4165 mol %, 0.3125 mol %, or 0.25 mol %. For the dilution studies on $[AuP(^tBu_{)3}]SbF_6$, $AuClP(^tBu)_3$ and $AgSbF_6$ were each added in 5 mol %, 2.5 mol %, 1.67 mol %, 1 mol %, 0.833 mol %, 0.625 mol %, and 0.5 mol %. The catalyst concentration was; thus, lowered by adding less catalyst whilst keeping the solvent volume 0.5 mL and the amount of substrate 50 µmol (11.8 mg). Stirring and heating to 60 °C; however, was done for 20 h instead of 5 h to obtain sufficient conversion in the experiments with very low catalyst concentrations.

### *3.4. Single Crystal X-ray Crystallography*

**Complex 5.** X-ray intensities were measured on a Bruker D8 Quest Eco diffractometer equipped with a Triumph monochromator (λ = 0.71073 Å) and a CMOS Photon 50 detector at a temperature of 150(2) K. Intensity data were integrated with the Bruker *APEX2* software [56]. Absorption correction and scaling was performed with *SADABS* [57]. The structures were solved using intrinsic phasing with the program *SHELXT* [56]. Least-squares refinement was performed with S*HELXL*-2013 [58] against $F^2$ of all reflections. Non-hydrogen atoms were refined with anisotropic displacement parameters. The H atoms were placed at calculated positions using the instructions AFIX 13, AFIX 43, or AFIX 137, with isotropic displacement parameters having values 1.2 or 1.5 times Ueq of the attached C atoms. $C_{39}H_{29}OP_2Au_2SbF_6$, $F_w$ = 1205.28, colorless block, 0.364 × 0.115 × 0.095 mm, monoclinic, $P2_1/c$ (No: 14)), $a$ = 13.9459(8), $b$ = 31.1012(19), $c$ = 10.9557(7) Å, β = 105.449(2)°, $V$ = 4580.2(5) Å$^3$, $Z$ = 4, $D_x$ = 1.951 g/cm$^3$, µ = 7.107 mm$^{-1}$. A total of 25854 reflections were measured up to a resolution of $(\sin \theta/\lambda)_{max}$ = 0.84 Å$^{-1}$. A total of 8204 reflections were unique ($R_{int}$ = 0.0557), of which 6409 were observed [$I > 2\sigma(I)$]. A total of 526 parameters were refined with 0 restraints. $R1/wR2$ [$I > 2\sigma(I)$]: 0.0439/0.0993. $R1/wR2$ [all refl.]: 0.0682/0.1135. S = 1.125. Residual electron density between −1.313 and 1.141 e/Å$^3$.

**Complexes 2 and 3.** All reflection intensities were measured at 110(2) K using a SuperNova diffractometer (equipped with Atlas detector) with Cu Kα radiation (λ = 1.54178 Å) under the program CrysAlisPro (Version 1.171.37.35 Agilent Technologies, 2014). The same program was used to refine the cell dimensions and for data reduction. The structure was solved with the program *SHELXS*-2014/7 (Sheldrick, 2015) and was refined on $F^2$ with *SHELXL*-2014/7 (Sheldrick, 2015). Analytical numeric absorption correction, using a multifaceted crystal model, was applied using CrysAlisPro. The temperature of the data collection was controlled using the system Cryojet (manufactured by Oxford Instruments). The H atoms were placed at calculated positions using the instructions AFIX 13, AFIX 43, or AFIX 137, with isotropic displacement parameters having values 1.2 or 1.5 times Ueq of the attached C atoms. **2**: The structure was partly disordered. The asymmetric unit contained a disordered mixture of lattice solvent molecule (CHCl3 and Acetone) at one site. The occupancy factors for the chloroform and acetone molecules were refined to 0.279(3) and 0.721(3), respectively. The crystal that was mounted on the diffractometer was twinned. The two twin components were related by a twofold axis along the reciprocal vector 0.9040a* − 0.0000b* − 0.4276c*. The BASF scale factor was refined to 0.3272(7). **3**: The structure was ordered. The crystal that was mounted on the diffractometer was twinned. The two twin components were related by a twofold axis along the reciprocal vector 0.0001a* + 0.0004b* + 1.0000c*. The BASF scale factor was refined to 0.4368(7).

CCDC 1893603 (5), 1894224 (2), and 1894225 (3) contain the supplementary crystallographic data for this paper (see Supplementary Materials). These data can be obtained free of charge from The Cambridge Crystallographic Data Centre via www.ccdc.cam.ac.uk/data_request/cif.

## 4. Conclusions

In summary, we demonstrate that the wide bite-angle diphosphine ligands, DBFPhos and DPEPhos, provide good platforms for the formation of catalytically relevant bis-gold complexes, featuring a bridging halide or alkynide ligand upon selective halide abstraction and follow-up

manipulation. Preorganization of both gold centers allows for selective σ,π-activation of functionalized alkynes. The well-defined dinuclear $Au^I$ complexes are excellent precatalysts for dual-gold catalysis involving selective σ,π-activation, inducing high regioselectivity in, for instance, the gold-catalyzed heterocyclization of urea **A**. Dilution experiments show that the dinuclear catalysts retain high selectivity at decreased catalyst loadings, unlike mononuclear Au(I) catalysts, which are typically employed for this reaction. These results underline the benefits of preorganization of gold centers to invoke selective substrate activation in dual-gold catalysis.

**Supplementary Materials:** The following are available online at http://www.mdpi.com/2304-6740/7/3/28/s1, Figure S1: $^{31}P\{^1H\}$ NMR spectrum of complex **1** ($CD_2Cl_2$, 298 K, 162 MHz), Figure S2: $^1H$ NMR spectrum of complex **1** ($CD_2Cl_2$, 298 K, 500 MHz), Figure S3: $^{13}C\{^1H\}$ NMR spectrum of complex **1** ($CD_2Cl_2$, 298 K, 126 MHz), Figure 4: Connectivity plot of complex **1**, Figure S5: $^{31}P\{^1H\}$ NMR spectrum of complex **2** ($CD_2Cl_2$, 298 K, 162 MHz), Figure S6: $^1H$ NMR spectrum of complex **2** ($CD_2Cl_2$, 298 K, 500 MHz), Figure S7: $^{13}C\{^1H\}$ NMR spectrum of complex **2** ($CD_2Cl_2$, 298 K, 126 MHz), Figure S8: $^{31}P\{^1H\}$ NMR spectrum of complex **3** ($CD_2Cl_2$, 298 K, 162 MHz), Figure S9: $^1H$ NMR spectrum of complex **3** ($CD_2Cl_2$, 298 K, 500 MHz), Figure S10: $^{13}C\{^1H\}$ NMR spectrum of complex **3** ($CD_2Cl_2$, 298 K, 126 MHz), Figure S11: $^{31}P\{^1H\}$ NMR spectrum of complex **4** ($CD_2Cl_2$, 298 K, 162 MHz), Figure S12: $^1H$ NMR spectrum of complex **4** ($CD_2Cl_2$, 298 K, 500 MHz), Figure S13: $^{13}C\{^1H\}$ NMR spectrum of complex **4** ($CD_2Cl_2$, 298 K, 126 MHz), Figure S14: $^{31}P\{^1H\}$ NMR spectrum of complex **5** ($CD_2Cl_2$, 298 K, 162 MHz), Figure S15: $^1H$ NMR spectrum of product **B** (98%) and **C** (2%) ($CDCl_3$, 298 K, 400 MHz), obtained by using complex **1** and two equivalents $AgSbF_6$, Figure S16: $^1H$ NMR spectrum of product **B** (100%) ($CDCl_3$, 298 K, 400 MHz), obtained by using complex **2** and two equivalents $AgSbF_6$, Figure S17: $^1H$ NMR spectrum of product **B** (97%) and **C** (3%) ($CDCl_3$, 298 K, 400 MHz), obtained by using complex **3** and one equivalent $AgSbF_6$, Figure S18: $^1H$ NMR spectrum of product **B** (95%) and **C** (5%) ($CDCl_3$, 298 K, 400 MHz), obtained by using complex **4** and one equivalent $AgSbF_6$, Figure S19: $^1H$ NMR spectrum of substrate **D** (acetone-$d_6$, 298 K, 300 MHz), Figure S20: $^1H$ NMR spectrum of product **E** (acetone-$d_6$, 298 K, 300 MHz), Figure S21: $^1H$ NMR spectrum of substrate **F** ($CDCl_3$, 298 K, 300 MHz), Figure S22: $^1H$ NMR spectrum of product **G** ($CDCl_3$, 298 K, 300 MHz); CIF and checkCIF data for complexes **2**, **3,** and **5**.

**Author Contributions:** Conceptualization, J.I.v.d.V.; funding acquisition, J.I.v.d.V.; investigation, M.L., V.V., and M.A.S.; supervision, J.I.v.d.V.; writing—original draft, M.L. and J.I.v.d.V.

**Funding:** This research was funded by the European Research Council (ERC) through Starting Grant 279097 (*EuReCat*) to J.I.v.d.V.

**Acknowledgments:** The authors thank Joost Reek for his interest in our work and Ed Zuidinga for ESI-MS measurements.

**Conflicts of Interest:** The authors declare no conflict of interest.

## References

1. Hashmi, A.S.K. Dual-Gold Catalysis. *Acc. Chem. Res.* **2014**, *47*, 864–876. [CrossRef] [PubMed]
2. Chiarucci, M.; Bandini, M. New developments in gold-catalyzed manipulation of inactivated alkenes. *Beilstein J. Org. Chem.* **2013**, *9*, 2586–2614. [CrossRef] [PubMed]
3. Ranieri, B.; Escofet, I.; Echavarren, A.M. Anatomy of gold catalysts: Facts and myths. *Org. Biomol. Chem.* **2015**, *13*, 7103–7118. [CrossRef] [PubMed]
4. Dorel, R.; Echavarren, A.M. Gold(I)-Catalyzed Activation of Alkynes for the Construction of Molecular Complexity. *Chem. Rev.* **2015**, *115*, 9028–9072. [CrossRef] [PubMed]
5. Wei, Y.; Shi, M. Divergent Synthesis of Carbo- and Heterocycles via Gold-Catalyzed Reactions. *ACS Catal.* **2016**, *6*, 2515–2524. [CrossRef]
6. Pflästerer, D.; Hashmi, A.S.K. Gold catalysis in total synthesis—Recent achievements. *Chem. Soc. Rev.* **2016**, *45*, 1331–1367. [CrossRef] [PubMed]
7. Jans, A.C.H.; Caumes, X.; Reek, J.N.H. Gold Catalysis in (Supra)Molecular Cages to Control Reactivity and Selectivity. *ChemCatChem* **2019**, *11*, 287–297. [CrossRef]
8. Cheong, P.H.-Y.; Morganelli, P.; Luzung, M.R.; Houk, K.N.; Toste, F.D. Gold-Catalyzed Cycloisomerization of 1,5-Allenynes via Dual Activation of an Ene Reaction. *J. Am. Chem. Soc.* **2008**, *130*, 4517–4526. [CrossRef] [PubMed]

9. Grirrane, A.; Garcia, H.; Corma, A.; Álvarez, E. Intermolecular [2 + 2] Cycloaddition of Alkyne-Alkene Catalyzed by Au(I) Complexes. What Are the Catalytic Sites Involved? *ACS Catal.* **2011**, *1*, 1647–1653. [CrossRef]
10. Hashmi, A.S.K.; Braun, I.; Nösel, P.; Schädlich, J.; Wieteck, M.; Rudolph, M.; Rominger, F. Simple Gold-Catalyzed Synthesis of Benzofulvenes—*gem*-Diaurated Species as "Instant Dual-Activation" Precatalysts. *Angew. Chem. Int. Ed.* **2012**, *51*, 4456–4460. [CrossRef] [PubMed]
11. Hashmi, A.S.K.; Braun, I.; Rudolph, M.; Rominger, F. The Role of Gold Acetylides as a Selectivity Trigger and the Importance of gem-Diaurated Species in the Gold-Catalyzed Hydroarylating-Aromatization of Arene-Diynes. *Organometallics* **2012**, *31*, 644–661. [CrossRef]
12. Ye, L.; Wang, Y.; Aue, D.H.; Zhang, L. Experimental and Computational Evidence for Gold Vinylidenes: Generation from Terminal Alkynes via a Bifurcation Pathway and Facile C–H Insertions. *J. Am. Chem. Soc.* **2012**, *134*, 31–34. [CrossRef] [PubMed]
13. Oonishi, Y.; Gómez-Suárez, A.; Martin, A.R.; Nolan, S.P. Hydrophenoxylation of Alkynes by Cooperative Gold Catalysis. *Angew. Chem. Int. Ed.* **2013**, *52*, 9767–9771. [CrossRef] [PubMed]
14. Højer Larsen, M.; Houk, K.N.; Hashmi, A.S.K. Dual Gold Catalysis: Stepwise Catalyst Transfer via Dinuclear Clusters. *J. Am. Chem. Soc.* **2015**, *137*, 10668–10676. [CrossRef] [PubMed]
15. Tkatchouk, E.; Mankad, N.P.; Benitez, D.; Goddard, W.A.; Toste, F.D. Two Metals Are Better Than One in the Gold Catalyzed Oxidative Heteroarylation of Alkenes. *J. Am. Chem. Soc.* **2011**, *133*, 14293–14300. [CrossRef] [PubMed]
16. Abadie, M.-A.; Trivelli, X.; Medina, F.; Capet, F.; Roussel, P.; Agbossou-Niedercorn, F.; Michon, C. Asymmetric Intramolecular Hydroamination of Alkenes in Mild and Wet Conditions—Structure and Reactivity of Cationic Binuclear Gold(I) Catalysts. *ChemCatChem* **2014**, *6*, 2235–2239. [CrossRef]
17. Serrano-Becerra, J.M.; Maier, A.F.G.; González-Gallardo, S.; Moos, E.; Kaub, C.; Gaffga, M.; Niedner-Schatteburg, G.; Roesky, P.W.; Breher, F.; Paradies, J. Mono- vs. Dinuclear Gold-Catalyzed Intermolecular Hydroamidation. *Eur. J. Org. Chem.* **2014**, 4515–4522. [CrossRef]
18. Hashmi, A.S.K.; Lauterbach, T.; Nösel, P.; Vilhelmsen, M.H.; Rudolph, M.; Rominger, F. Dual Gold Catalysis: σ,π-Propyne Acetylide and Hydroxyl-Bridged Digold Complexes as Easy-To-Prepare and Easy-To-Handle Precatalysts. *Chem. Eur. J.* **2012**, *19*, 1058–1065. [CrossRef] [PubMed]
19. Vreeken, V.; Broere, D.L.J.; Jans, A.C.H.; Lankelma, M.; Reek, J.N.H.; Siegler, M.A.; van der Vlugt, J.I. Well-Defined Dinuclear Gold Complexes for Preorganization-Induced Selective Dual Gold Catalysis. *Angew. Chem. Int. Ed.* **2016**, *55*, 10042–10046. [CrossRef] [PubMed]
20. Vreeken, V.; Siegler, M.A.; van der Vlugt, J.I. Controlled Interconversion of a Dinuclear Au Species Supported by a Redox-Active Bridging PNP Ligand Facilitates Ligand-to-Gold Electron Transfer. *Chem. Eur. J.* **2017**, *23*, 5585–5594. [CrossRef] [PubMed]
21. Kamer, P.C.J.; van Leeuwen, P.W.N.M. *Phosphorus(III) Li Gands in Homogeneous Catalysis: Design and Synthesis*; Wiley: Chichester, UK, 2012.
22. Van Leeuwen, P.W.N.M.; Kamer, P.C.J. Featuring Xantphos. *Catal. Sci. Technol.* **2018**, *8*, 26–113. [CrossRef]
23. Kamer, P.C.J.; van Leeuwen, P.W.N.M.; Reek, J.N.H. Wide Bite Angle Diphosphines: Xantphos Ligands in Transition Metal Complexes and Catalysis. *Acc. Chem. Res.* **2001**, *34*, 895–904. [CrossRef] [PubMed]
24. Kranenburg, M.; van der Burgt, Y.E.M.; Kamer, P.C.J.; van Leeuwen, P.W.N.M.; Goubitz, K.; Fraanje, J. New Diphosphine Ligands Based on Heterocyclic Aromatics Inducing Very High Regioselectivity in Rhodium-Catalyzed Hydroformylation: Effect of the Bite Angle. *Organometallics* **1995**, *14*, 3081–3089.
25. Van der Vlugt, J.I.; van Duren, R.; Batema, G.D.; den Heeten, R.; Meetsma, A.; Fraanje, J.; Goubitz, K.; Kamer, P.C.J.; van Leeuwen, P.W.N.M.; Vogt, D. Platinum Complexes of Rigid Bidentate Phosphine Ligands in the Hydroformylation of 1-Octene. *Organometallics* **2005**, *24*, 5377–5382. [CrossRef]
26. Van Duren, R.; van der Vlugt, J.I.; Mills, A.M.; Spek, A.L.; Vogt, D. Platinum-catalyzed hydroformylation of terminal and internal octenes. *Dalton Trans.* **2007**, 1053–1059. [CrossRef] [PubMed]
27. Czauderna, C.F.; Cordes, D.B.; Slawin, A.M.Z.; Müller, C.; van der Vlugt, J.I.; Vogt, D.; Kamer, P.C.J. Synthesis and reactivity of chiral wide bite angle hybrid diphosphorus ligands. *Eur. J. Inorg. Chem.* **2014**, 1797–1810. [CrossRef]
28. Czauderna, C.F.; Jarvis, A.G.; Heutz, F.J.L.; Cordes, D.B.; Slawin, A.M.Z.; van der Vlugt, J.I.; Kamer, P.C.J. Chiral Wide-Bite-Angle Diphosphine Ligands: Synthesis, Coordination Chemistry, and Application in Pd-Catalyzed Allylic Alkylation. *Organometallics* **2015**, *34*, 1608–1618. [CrossRef]

29. Czauderna, C.F.; Slawin, A.M.Z.; Cordes, D.B.; van der Vlugt, J.I.; Kamer, P.C.J. P-stereogenic wide bite angle diphosphine ligands. *Tetrahedron* **2019**, *75*, 47–56. [CrossRef]
30. De la Riva, H.; Nieuwhuyzen, M.; Mendicute Fierro, C.; Raithby, P.R.; Male, L.; Lagunas, M.C. A New Type of Luminescent Alkynyl $Au_4Cu_2$ Cluster. *Inorg. Chem.* **2006**, *45*, 1418–1420. [CrossRef] [PubMed]
31. Pintado-Alba, A.; de la Riva, H.; Nieuwhuyzen, M.; Bautista, D.; Raithby, P.R.; Sparkes, H.A.; Teat, S.J.; López-de-Luzuriaga, J.M.; Lagunas, M.C. Effects of diphosphine structure on aurophilicity and luminescence in Au(I) complexes. *Dalton Trans.* **2004**, 3459–3467. [CrossRef] [PubMed]
32. Partyka, D.V.; Updegraff III, J.B.; Zeller, M.; Hunter, A.D.; Gray, T.G. Gold(I) halide complexes of bis(diphenylphosphine)diphenyl ether ligands: A balance of ligand strain and non-covalent interactions. *Dalton Trans.* **2010**, *39*, 5388–5397. [CrossRef] [PubMed]
33. Glebko, N.; Dau, T.M.; Melnikov, A.S.; Grachova, E.V.; Solovyev, I.V.; Belyaev, A.; Karttunen, A.J.; Koshevoy, I.O. Luminescence Thermochromism of Gold(I) Phosphane–Iodide Complexes: A Rule or an Exception? *Chem. Eur. J.* **2018**, *24*, 3021–3029. [CrossRef] [PubMed]
34. Jobbágy, C.; Baranai, P.; Marsi, G.; Rácz, B.; Li, L.; Naumov, P.; Deák, A. Novel gold(I) diphosphine-based dimers with aurophilicity triggered multistimuli light-emitting properties. *J. Mater. Chem. C* **2016**, *4*, 10253–10264. [CrossRef]
35. Jobbágy, C.; Baranai, P.; Szabó, P.; Holczbauer, T.; Rácz, B.; Li, L.; Naumov, P.; Deák, A. Unexpected formation of a fused double cycle trinuclear gold(I) complex supported by ortho-phenyl metallated aryl-diphosphine ligands and strong aurophilic interactions. *Dalton Trans.* **2016**, *45*, 12569–12575. [CrossRef] [PubMed]
36. Baranai, P.; Marsi, G.; Hamza, A.; Jobbágy, C.; Deák, A. Structural characterization of dinuclear gold(I) diphosphine complexes with anion-triggered luminescence. *Struct. Chem.* **2015**, *26*, 1377–1387. [CrossRef]
37. Ito, H.; Saito, T.; Miyahara, T.; Zhong, C.; Sawamura, M. Gold(I) Hydride Intermediate in Catalysis: Dehydrogenative Alcohol Silylation Catalyzed by Gold(I) Complex. *Organometallics* **2009**, *28*, 4829–4840. [CrossRef]
38. Deák, A.; Megyes, T.; Tárkányi, G.; Király, P.; Biczók, L.; Pálinkás, G.; Stang, P.J. Synthesis and Solution- and Solid-State Characterization of Gold(I) Rings with Short Au···Au Interactions. Spontaneous Resolution of a Gold(I) Complex. *J. Am. Chem. Soc.* **2006**, *128*, 12668–12670. [CrossRef] [PubMed]
39. Schmidbaur, H.; Schier, A. A briefing on aurophilicity. *Chem. Soc. Rev.* **2008**, *37*, 1931–1951. [CrossRef] [PubMed]
40. Walters, D.T.; England, K.R.; Ghiassi, K.B.; Semma, F.Z.; Olmstead, M.M.; Balch, A.L. Steric effects and aurophilic interactions in crystals of $Au_2$(μ-1,2-bis(diphenylphosphino)ethane)$X_2$ and $Au_2$(μ-1,2-bis(dicyclohexylphosphino)ethane)$X_2$ (X = Cl, Br, I). *Polyhedron* **2016**, *117*, 535–541. [CrossRef]
41. Mir, M.H.; Ong, J.X.; Kole, G.K.; Tan, G.K.; McGlinchey, M.J.; Wu, Y.; Vittal, J.J. Photoreactive gold(I) macrocycles with diphosphine and *trans*,*trans*-muconate ligands. *Chem. Commun.* **2011**, *47*, 11633–11635. [CrossRef] [PubMed]
42. Grirrane, A.; Álvarez, E.; García, H.; Corma, A. Deactivation of Cationic $Cu^I$ and $Au^I$ Catalysts for $A^3$ Coupling by $CH_2Cl_2$: Mechanistic Implications of the Formation of Neutral $Cu^I$ and $Au^I$ Chlorides. *Angew. Chem. Int. Ed.* **2014**, *53*, 7253–7258. [CrossRef] [PubMed]
43. Phillips, N.; Dodson, T.; Tirfoin, R.; Bates, J.I.; Aldridge, S. Expanded-Ring *N*-Heterocyclic Carbenes for the Stabilization of Highly Electrophilic Gold(I) Cations. *Chem. Eur. J.* **2014**, *20*, 16721–16731. [CrossRef] [PubMed]
44. Zhu, Y.; Day, C.S.; Zhang, L.; Hauser, K.J.; Jones, A.C. A Unique Au–Ag–Au Triangular Motif in a Trimetallic Halonium Dication: Silver Incorporation in a Gold(I) Catalyst. *Chem. Eur. J.* **2013**, *19*, 12264–12271. [CrossRef] [PubMed]
45. Homs, A.; Escofet, I.; Echavarren, A.M. On the Silver Effect and the Formation of Chloride-Bridged Digold Complexes. *Org. Lett.* **2013**, *15*, 5782–5785. [CrossRef] [PubMed]
46. Yam, V.W.W.; Chan, C.-L.; Cheung, K.-K. Synthesis and photophysics of dinuclear gold(I) thiolates of bis(diphenylphosphino)-alkyl- and -aryl-amines. Crystal structure of [$Au_2${$Ph_2PN(C_6H_{11})PPh_2$}($SC_6H_4$F-*p*)$_2$]. *J. Chem. Soc. Dalton Trans.* **1996**, 4019–4022. [CrossRef]
47. Jones, P.G.; Sheldrick, G.M.; Uson, R.; Lapuna, A. μ-Chloro-bis(triphenylphosphine) digold(I) perchlorate dichloromethane solvate. *Acta Cryst. B* **1980**, *36*, 1486. [CrossRef]

48. Hamel, A.; Mitzel, N.W.; Schmidbaur, H. Metallophilicity: The Dimerization of Bis[(triphenylphosphine)gold(I)]chloronium Cations. *J. Am. Chem. Soc.* **2001**, *123*, 5106–5107. [CrossRef]
49. Gimeno, A.; Cuenca, A.B.; Suárez-Pantiga, S.; Ramírez de Arellano, C.; Medio-Simón, M.; Asensio, G. Competitive Gold-Activation Modes in Terminal Alkynes: An Experimental and Mechanistic Study. *Chem. Eur. J.* **2014**, *20*, 683–688. [CrossRef] [PubMed]
50. Gramage-Doria, R.; Hessels, J.; Leenders, S.H.A.M.; Tröppner, O.; Dürr, M.; Ivanović-Burmazović, I.; Reek, J.N.H. Gold(I) Catalysis at Extreme Concentrations Inside Self-Assembled Nanospheres. *Angew. Chem. Int. Ed.* **2014**, *53*, 13380–13384. [CrossRef] [PubMed]
51. Wang, Q.Q.; Gonell, S.; Leenders, S.H.A.M.; Tröppner, O.; Dürr, M.; Ivanović-Burmazović, I.; Reek, J.N.H. Self-assembled nanospheres with multiple endohedral binding sites pre-organize catalysts and substrates for highly efficient reactions. *Nat. Chem.* **2016**, *8*, 225–230. [CrossRef] [PubMed]
52. Ye, D.; Wang, J.; Zhang, X.; Zhou, Y.; Ding, X.; Feng, E.; Sun, H.; Liu, G.; Jiang, H.; Liu, H. Gold-catalyzed intramolecular hydroamination of terminal alkynes in aqueous media: Efficient and regioselective synthesis of indole-1-carboxamides. *Green Chem.* **2009**, *11*, 1201–1208. [CrossRef]
53. Jiang, Y.; Wei, Y.; Tang, X.Y.; Shi, M. Gold(I)-Catalyzed Selective Heterocyclization of Propargylic Thioureas: Mechanistic Study of Competitive Gold-Activation Mode. Gold(I)-Catalyzed Selective Heterocyclization of Propargylic Thioureas: Mechanistic Study of Competitive Gold-Activation Mode. *Chem. Eur. J.* **2015**, *21*, 7675–7681. [CrossRef] [PubMed]
54. Praveen, C.; Perumal, P. Revisiting the Gold-Catalyzed Dimerization of 2-Ethynylanilines: A Room-Temperature and Silver-Free Protocol for the Synthesis of Multifunctional Quinolines. *Synthesis* **2016**, *48*, 855–864. [CrossRef]
55. Varela-Fernández, A.; Varela, J.A.; Saá, C. Formation of Indoles, Dihydroisoquinolines, and Dihydroquinolines by Ruthenium-Catalyzed Heterocyclizations. *Synthesis* **2012**, *44*, 3285–3295.
56. Bruker. *APEX2 Software*; Bruker: Madison, WI, USA, 2014.
57. Sheldrick, G.M. *SADABS*; Universität Göttingen: Lower Saxony, Germany, 2008.
58. Sheldrick, G.M. *SHELXL2013*; University of Göttingen: Lower Saxony, Germany, 2013.